Chem

CellPress

Article

Terpenoid-based high-performance polyester with tacticity-independent crystallinity and chemical circularity

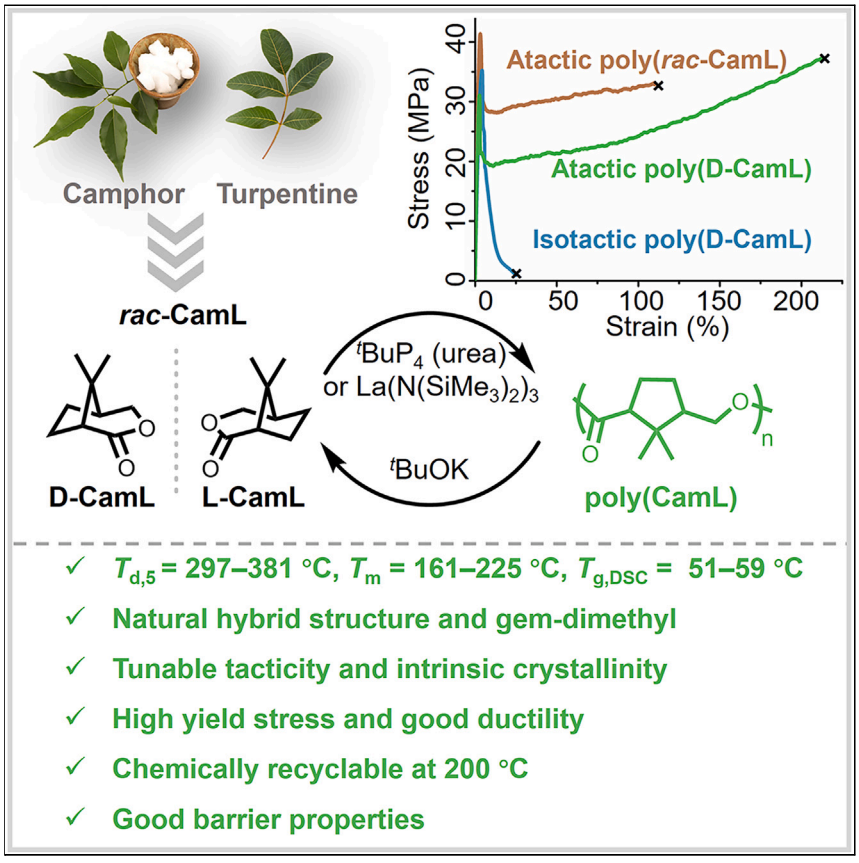

Plastic pollution is a major global crisis. Sustainable solutions typically involve developing polymers with closed-loop chemical recyclability and using renewable monomers. Herein, we developed a terpenoid-derived, chemically recyclable polyester with mechanical and thermal properties comparable to, or better than, those of poly(lactic acid) (PLA). Permeability experiments further indicate that this polyester is suitable for packaging applications.

Zhitao Hu, Simone N. Bernsten, Changxia Shi, Ainara Sangroniz, Eugene Y.-X. Chen, Garret M. Miyake

garret.miyake@colostate.edu

Highlights

A terpenoid-derived and chemically recyclable polyester is developed

The bio-derived polyester has comparable thermal properties to those of PLA

The sustainable polyester is tough, ductile, and intrinsically crystalline

Hu et al., Chem *10*, 3040–3054
October 10, 2024
https://doi.org/10.1016/j.chempr.2024.05.024

CellPress

Chem

Article

Terpenoid-based high-performance polyester with tacticity-independent crystallinity and chemical circularity

Zhitao Hu,[1,3] Simone N. Bernsten,[1,3] Changxia Shi,[1] Ainara Sangroniz,[2] Eugene Y.-X. Chen,[1] and Garret M. Miyake[1,4,*]

SUMMARY

The development of chemically circular, bio-based polymers is an urgently needed solution to combat the plastic waste crisis. However, the most prominent, commercially implemented bio-based aliphatic polyester, poly(lactic acid) (PLA), is brittle, therefore largely limiting its broad applications. Herein, we introduce a class of aliphatic polyesters produced through the ring-opening polymerization (ROP) of (1*R*,5*S*)-8,8-dimethyl-3-oxabicyclo[3.2.1]octan-2-one (D-CamL) and the racemic mixture (*rac*-CamL), which exhibit superior material properties relative to PLA. A metal-based or organic catalyst was used for the modulation of polymer tacticity. Notably, regardless of tacticity, poly(CamL) exhibits intrinsic crystallinity, resulting in polyesters with high yield stress (24–39 MPa), high Young's modulus (1.36–2.00 GPa), tunable fracture strains (6%–218%), and high melting temperatures (161°C–225°C). Importantly, poly(CamL) can be chemically recycled to monomer in high yield, and virgin-quality poly(CamL) is obtained after repolymerization. Overall, poly(CamL) represents a new class of bio-derived and chemically circular high-performance polyesters.

INTRODUCTION

Plastic products have become ubiquitous and irreplaceable in modern life, but linear life cycles and poor end-of-life options result in significant environmental issues such as waste accumulation and consumption of finite resources.[1,2] Plastic recycling is critical, but traditional mechanical recycling methods yield materials with diminished properties and reduced value.[3,4] To address the shortcomings of mechanical recycling, alternative recycling strategies that enable the retention of material properties are needed.[5] Among these approaches, closed-loop chemical recycling is a desirable technology in which polymeric materials can be efficiently deconstructed into their starting monomers or oligomers and repolymerized into chemically identical, virgin-like polymer materials.[6–10]

In addition to chemical circularity, polymer sustainability can further be enhanced by the use of bio-derived monomers and feedstocks, especially those that do not come from food sources.[11] Among chemically recyclable bio-derived polymers, poly(lactic acid) (PLA) has become particularly prevalent given its relatively low cost,[12] processability,[13] chemical recyclability,[14,15] and generally desirable properties.[16,17] The crystalline and amorphous states of PLA are strongly dependent on the stereochemistry of the polymer backbone, with isotactic and syndiotactic PLA exhibiting crystallinity. Syndiotactic PLA has a lower glass-transition temperature (T_g) and melting

THE BIGGER PICTURE

Plastic pollution is currently one of the world's foremost environmental problems. Single-use plastics often end up in landfills, as pollution, are incinerated, or are mechanically recycled. Mechanical recycling is a desirable option, but it results in degraded, lower-value materials. Attractive approaches to sustainable plastics involve developing polymeric materials that exhibit closed-loop chemical recyclability (also known as chemical circularity) and using renewably sourced monomers instead of petroleum-derived monomers. Herein, we report a terpenoid-derived, chemically recyclable plastic that is intrinsically crystalline, strong, ductile, and thermally stable and also exhibits barrier properties suitable for packaging applications. Overall, this aliphatic polyester platform provides promise as a renewably sourced and chemically recyclable plastic that exhibits material properties comparable to, or exceeding, those of the most common bio-derived plastic, poly(lactic acid) (PLA).

temperature (T_m) but a higher crystallization temperature (T_c) than isotactic PLA.[18] Regardless of being crystalline or amorphous, the low elongation at break (ϵ_B < 10%) of PLA and its high water and oxygen permeability ($P\ O_2$) limit the use of PLA materials in packaging applications.[17,19,20] In terms of the recycling of isotactic poly(L-lactic acid) (PLLA), the selective depolymerization to enantiopure monomer can be challenging.[14,15] As such, the shortcomings of PLA inspired us to explore new bio-derived polymers that may have materials properties comparable to or exceeding those of PLA.

Several notable innovations toward chemically recyclable plastics have been recently made. For example, 1,3-dioxolane (DXL), made from industrial feedstocks formaldehyde and ethylene glycol, is regarded as a green building block for recyclable plastic and can be polymerized by cationic ring-opening polymerization (ROP) to yield high molecular weight poly(DXL) with potential for use as a packaging material. Poly(DXL) can be chemically recycled back to DXL, demonstrating an example of a successful circular plastic economy.[21,22] However, the low T_m of poly(DXL) (∼60°C) may limit its application in certain applications. Similarly, polymer made from the bio-derived monomer δ-valerolactone (VL) also has a low T_m (∼57°C). In order to make chemically recyclable, bio-based polymers that are tolerant to higher temperatures, structural modification of commercially available monomers can be a promising platform.[23] One example of such structural modification is the addition of geminal dialkyl (gem-dialkyl) functionality. In the case of VL, gem-disubstitution yields a gem-diakyl-substituted polymer, poly(VL^{R2}), possessing a high T_m (∼140°C). Additionally, poly(VL^{R2}) has good mechanical properties (ϵ_B could reach 322%) and a reduced ceiling temperature ($T_{ceiling}$, defined as equilibrium temperature between polymerization and depolymerization) from 298°C for VL to 67°C for VL^{R2} at 1 M.[24] The low ceiling temperature of poly(VL^{R2}) makes it easier to thermally depolymerize than unsubstituted poly(VL), which can be explained by the fact that gem-dialkyl substitution enables harnessing of the Thorpe-Ingold effect[25,26] to promote ring closure during depolymerization, thereby enabling facile recovery of monomer. Polyhydroxyalkanoates (PHAs) are another important class of bio-derived polyesters with the potential to serve as analogs for PLA. However, their general thermal instability, and mechanical brittleness limit materials properties, while their propensity for α-hydrogen (H) elimination render them difficult to efficiently depolymerize back to their starting lactones.[27] Gem-dialkyl-substitution at the α-position of poly(3-hydroxybutyrate) (P3HB) produces poly(3-hydroxy-2,2-dialkylbutyrate) [P3H(alkyl)$_2$B], which exhibits the unique property of intrinsic crystallinity, can undergo melt processing, and can be recycled back to the corresponding lactone by NaOH at 210°C. The ϵ_B could reach 517% after gem-disubstitution, thus displaying significant improvement in mechanical properties relative to the unsubstituted polymer (ϵ_B, ∼4%).[28] These reports demonstrate that gem-dialkyl-substitution can increase the materials properties and help realize the closed-loop recycling of bio-based polymers under mild conditions.

In addition to the gem-dialkyl-substitution strategy applied in monomer design, a recently developed hybrid monomer (or hybrid bicyclic monomer) strategy results in increased ease of chemical recycling as well as increased T_m and T_g.[29–32] Hybrid monomers combine the structures of monomers possessing a high ring-strain and low $T_{ceiling}$, where structural motifs imparting high ring-strain facilitate the facile polymerization of the hybrid monomer, while motifs imparting a low $T_{ceiling}$ allow for efficient depolymerization. It is also noteworthy that the bridged bicyclic structure of the hybrid monomer facilitates depolymerization to selectively yield the *cis*-configuration monomer. With gem-dialkyl-substitution and hybrid monomer

[1]Department of Chemistry, Colorado State University, Fort Collins, CO 80523-1872, USA

[2]POLYMAT and Department of Polymers and Advanced Materials: Physics, Chemistry and Technology, Faculty of Chemistry, University of the Basque Country UPV/EHU, Paseo Manuelde Lardizábal 3, 20018 Donostia-San Sebastián, Spain

[3]These authors contributed equally

[4]Lead contact

*Correspondence: garret.miyake@colostate.edu

https://doi.org/10.1016/j.chempr.2024.05.024

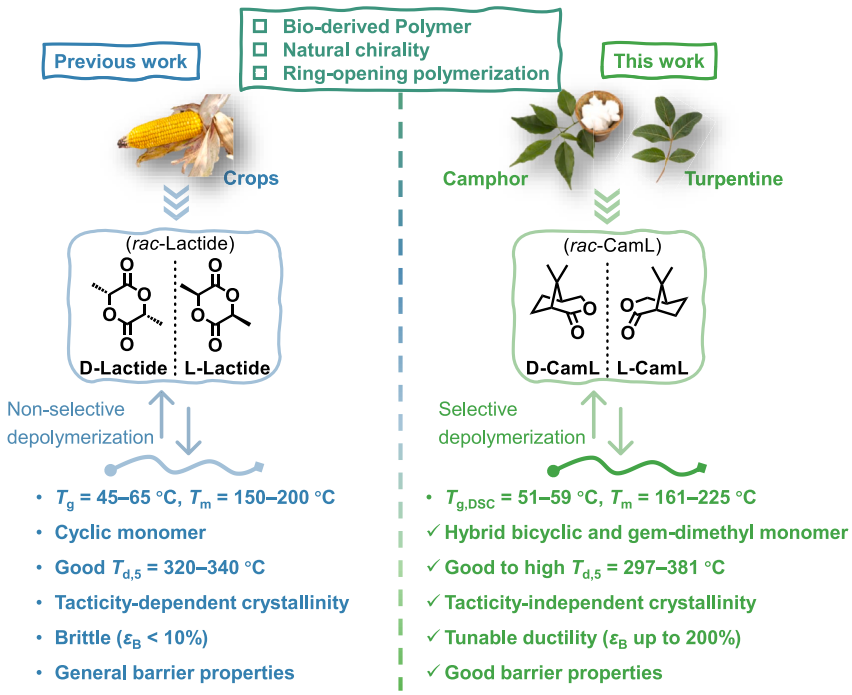

Scheme 1. Comparison between PLA and poly(CamL)

design strategies in mind, we hypothesized that terpenes or terpenoids would be suitable structures for constructing recyclable polyesters merging natural hybrid and gem-dialkyl-substitution approaches.[33,34] Terpene- and terpenoid-based polymers are relatively well studied, with many polymers possessing high T_g (70°C, 130°C) or high strength at break (70 MPa), but most are amorphous even if the isotactic polymer is obtained.[35–41] As such, the structural modification of terpenes or terpenoids for developing high-performance polymer materials is warranted. In the realm of terpenes and terpenoids, camphor is widely used in daily life and organic synthesis.[42–44] Similar to lactide, the monomer unit of PLA (Scheme 1), optically pure D-camphor ((1*R*,4*R*)-bornan-2-one), can be isolated from biomass, while the racemic mixture of camphor can be obtained through chemical synthesis from α-pinene (obtained from turpentine).[45] The molecular weights of previously reported camphor-derived polymers by condensation polymerization have not exceeded 20 kDa and are brittle materials (ϵ_B < 15%), which limits their application,[46–48] while ROP is more successful for producing higher molecular weight polymers.[49,50] The presence of a methyl group on the bridgehead carbon in the backbone of these polymers impedes their ability to crystallize and only amorphous polymer is obtained, while their T_g is higher than room temperature and polymers produced from camphor are rigid at room temperature.[46]

To broaden the application of terpene- or terpenoid-based polymers, we sought to use the structural modification strategy to design a camphor-based polymer that exhibited crystallinity and high-performance materials properties. We realized that the hybrid and gem-dimethyl structural motifs naturally occurring in camphor should be retained, but the monomethyl group on the bridgehead carbon should be removed to enable crystallization. Ultimately, the proposed lactone, (1*R*,5*S*)-8,8-dimethyl-3-oxabicyclo[3.2.1]octan-2-one (D-CamL) and the racemic mixture (*rac*-CamL or DL-CamL) (Schemes 1 and S1), were obtained. Both D-CamL and *rac*-CamL were

Table 1. Polymerization results of D-CamL

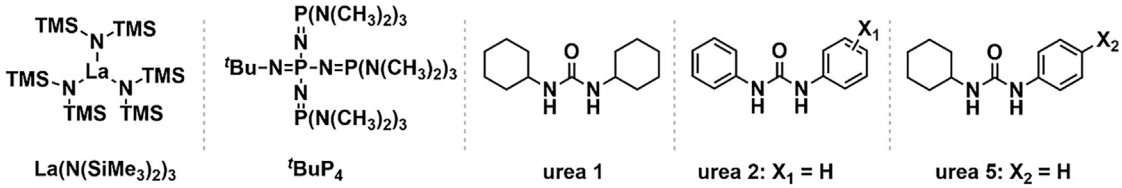

Run	Catalyst	Time (h)	Conv. (%)[a]	M_w (kDa)[b]	$Đ$[b]	T_g (°C)[c]	T_m (°C)[c]	ΔH_f (J/g)[c]	*cis*/*trans* (%/%)[d]
1	$La(N(SiMe_3)_2)_3$	2.0	68	9.80	1.30	N/A	186/216	29.0	100/0
2	Common bases[e]	24	N/A	N/A	N/A	N/A	N/A	N/A	N/A
3	$^tBuP_4$	1.0	88	34.5	1.50	58	169	30.6	61/39
4	$^tBuP_4$/urea	24	37	11.1	1.31	N/A	N/A	N/A	70/30
5	$^tBuP_4$/TU	24	N/A	N/A	N/A	N/A	N/A	N/A	N/A
6	$^tBuP_4$/urea 1	1.0	89	27.5	1.48	53	161	30.2	60/40
7	$^tBuP_4$/urea 2[f]	20	55	16.0	2.06	59	171	21.9	77/23
8	$^tBuP_4$/urea 3	80	41	14.4	1.33	N/A	170/195	27.3	92/8
9	$^tBuP_4$/urea 4	80	48	17.8	1.60	51	164/199	26.0	88/12
10	$^tBuP_4$/urea 5	6.0	96	24.2	1.77	59	188	25.0	67/33
11	$^tBuP_4$/urea 6	3.5	91	28.6	1.80	58	174	25.3	64/36

Conditions: conducted in THF at room temperature, except **Run 1** conducted in toluene at 100°C, initiated by BnO^-, and monomer concentration was 100 mg D-CamL in 200 μL THF, [M]:[BnOH]:[Cat.] = 100:1:1 except **Run 1** [M]:[BnOH]:[Cat.] = 70:1:1.

[a]Monomer conversions determined by ^1H NMR of the crude solution in $CDCl_3$ after quenching with benzoic acid.

[b]Weight-average molecular weights (M_w) and dispersity ($Đ = M_w/M_n$) determined by gel-permeation chromatography (GPC) coupled with light scattering at 40°C in $CHCl_3$.

[c]T_g, T_m, and heat of fusion (ΔH_f) measured by differential scanning calorimetry (DSC) using the second heating scan at a rate of 10°C min^{-1}.

[d]Measured by the carbonyl region of ^{13}C NMR in $CDCl_3$.

[e]Catalysts summarized in **Run 2**: DBU, TBD, and $^tBuP_2$.

[f]Reaction was stopped after 20 h because the mixture solidified. Note: ^1H NMR spectra, ^{13}C NMR spectra, thermogravimetric analysis (TGA) results, and DSC results can be found in Figures S3–S14.

polymerized via ROP to relatively high molecular weight. Thanks to the hybrid and gem-dimethyl structure in the CamL repeat unit, poly(CamL) has intrinsic crystallinity and exhibits similar thermal properties and yield stress to PLA, but with higher ϵ_B and lower water and $P\,O_2$. Furthermore, the closed-loop recycling of poly(CamL) could be easily performed under mild conditions (Scheme 1).

RESULTS AND DISCUSSION

Monomer design and polymerization

The D-camphor-derived lactone produced directly from the Baeyer-Villiger oxidation of D-camphor was not polymerizable under various conditions investigated (Table S1). We hypothesized that the α-methyl group inhibited the polymerization, presumably due to the steric hindrance of the methyl group in proximity to the carbonyl group. As such, we synthesized a D-camphor lactone derivative (D-CamL) devoid of the methyl group on the bridgehead carbon to investigate the polymerization of this monomer.

Initial attempts at the ROP of D-CamL used tris[N,N-bis(trimethylsilyl)amide] lanthanum [$La(N(SiMe_3)_2)_3$] as the catalyst, which has demonstrated success with benzyl alcohol as the initiator. Using $La(N(SiMe_3)_2)_3$ to catalyze the polymerization of D-CamL was only successful at elevated temperatures, achieving 68% conversion at 100°C after 2 h (M_w = 9.80 kDa, Table 1, **Run 1**). Given that $La(N(SiMe_3)_2)_3$ is

slightly expensive, tin octanoate [$Sn(Oct)_2$] was investigated as an alternative catalyst. However, when $Sn(Oct)_2$ was used for the polymerization of D-CamL at 100°C, there was no monomer conversion after 8 h (Table S2). Encouraged by the successful initial polymerization of D-CamL by $La(N(SiMe_3)_2)_3$, we explored organic catalysts. A series of common compounds (Table 1, **Run 2**) were investigated for the ROP of D-CamL, including 1,8-diazabicyclo(5.4.0)undec-7-ene (DBU), 1,5,7-triazabicyclo 4.4.0 dec-5-ene (TBD), and 1-tert-butyl-2,2,4,4,4-pentakis(dimethylamino)-2λ^5,4λ^5-catenadi(phosphazene) (^{t}BuP$_2$), but none of the initial attempts at the bases-mediated ROP of D-CamL were successful. Given that all compounds investigated are basic enough to deprotonate the initiator, we hypothesized that the polymerization of D-CamL could only proceed when the ion pair (formed through H-bonding) between the protonated catalyst and propagating chain ends is sufficiently weak.[51–53]

To test this hypothesis, 1-tert-butyl-4,4,4-tris(dimethylamino)-2,2-bis[tris(dimethylamino)-phosphoranylidenamino]-2λ,^{5}4λ^5-catenadi(phosphazene) (^{t}BuP$_4$, p$K_{a,\ ACN}$ = 42.7) was investigated and in 1 h successful conversion of monomer to polymer (88%) was observed (M_w = 34.5 kDa, Table 1, **Run 3**), supporting the hypothesis that the ion pair [^{t}BuP$_4$-H$^+$…O$^-$] must be weak enough for polymerization to proceed.

The polymerization solvent was subsequently investigated to achieve higher monomer conversion and greater polymerization control. In comparing poly(D-CamL) synthesized in acetonitrile (ACN), dimethylformamide (DMF), and toluene with poly(D-CamL) synthesized in tetrahydrofuran (THF), we found that there was no conversion of monomer in ACN, higher dispersity in DMF ($Đ$ = 1.96 in DMF, $Đ$ = 1.50 in THF), and much lower conversion of monomer in toluene (51% after 1 h). Therefore, THF was selected as the polymerization solvent moving forward (Table 1, **Run 3**, and Table S3). To assess the control over the polymerization of D-CamL catalyzed by ^{t}BuP$_4$, monomer conversion and polymer molecular weight were monitored over reaction time. Pseudo-first-order kinetics with respect to monomer (R^2 = 0.990, Figure S15A) were observed and polymer molecular weight increased linearly as a function of conversion (R^2 = 0.973, Figure S15B). Matrix-assisted laser desorption/ionization time-of-flight (MALDI-TOF) of poly(D-CamL) (Table 1, **Run 3**) supported the notion that the polymerization of D-CamL was initiated by BnO$^-$ (Figure S15C). However, a cyclic polymer chain could be seen, with low molecular weight species in the MALDI-TOF mass spectrum (Figures S15C and S15D) of poly(D-CamL) indicating that intramolecular transesterification occurred during the polymerization process, thereby limiting polymerization control and resulting in increased polymer dispersity. When polymerization kinetics, molecular weight trends, and polymer structural analysis are considered collectively, the ROP of D-CamL catalyzed by ^{t}BuP$_4$ is not well controlled. We conclude that control was limited by secondary transesterification reactions, where intramolecular transesterification could result in the formation of cyclic polymer chains.

Binary catalyst system

When comparing the ^{13}C NMR spectra of poly(D-CamL) synthesized using $La(N(SiMe_3)_2)_3$ and ^{t}BuP$_4$ (Figure 1A), it was deduced that the use of $La(N(SiMe_3)_2)_3$ resulted in isotactic poly(D-CamL) (Table 1, **Run 1**) with full *cis*-structure, while the use of ^{t}BuP$_4$ resulted in atactic poly(D-CamL) (Table 1, **Run 3**) with a *cis*/*trans* ratio of 61/39. The carbonyl region of the ^{13}C NMR spectrum of poly(D-CamL) (Table 1, **Run 1**) showed only one peak indicating isotactic polymer, while the ^{13}C NMR spectrum of poly(D-CamL) (Table 1, **Run 3**) showed two separated peaks indicating

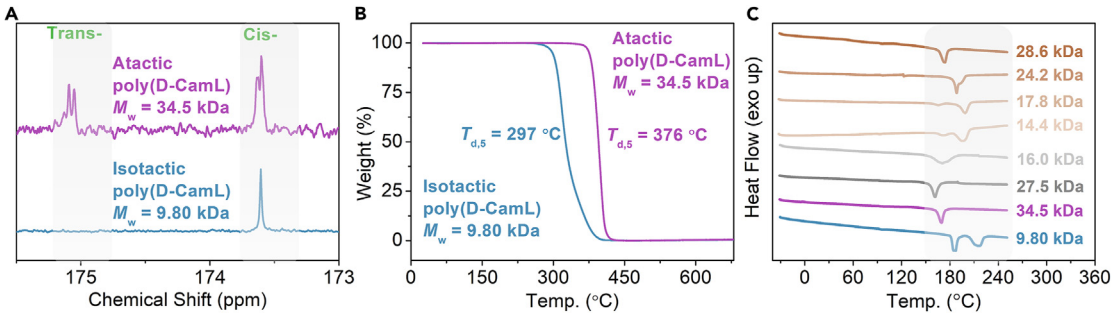

Figure 1. Properties of poly(D-CamL) prepared with different catalysts

(A) ^{13}C NMR ($CDCl_3$, 23°C) spectra of the **Run 1** (blue line, isotactic) and **Run 3** (purple line, atactic) in $CDCl_3$.

(B) TGA curves of the **Run 1** (blue line, isotactic) and **Run 3** (purple line, atactic).

(C) DSC profiles of the polymers came from **Runs 1**, **3**, and **6–11**, showing the second heating scans at 10°C/min.

non-uniformity in the stereoregularity. We hypothesized that the formation of atactic poly(D-CamL) resulted from epimerization of the bridgehead carbon near to the carbonyl group in the presence of the superbase $^{t}BuP_4$ (Scheme S2). To test this hypothesis, purified isotactic poly(D-CamL) (Table 1, **Run 1**) was treated with $^{t}BuP_4$ in THF; after stirring for 2 h, atactic poly(D-CamL) with a *cis*/*trans* = 60/40 was produced (Figure S16).

The thermal properties of the polymers possessing different tacticity were investigated. thermogravimetric analysis (TGA) of isotactic poly(D-CamL) (Table 1, **Run 1**) and atactic poly(D-CamL) (Table 1, **Run 3**) (Figure 1B) demonstrated that isotactic poly(D-CamL) ($T_{d,5}$ = 297°C, defined by the temperature at 5% weight loss) decomposes at a much lower temperature than atactic poly(D-CamL) ($T_{d,5}$ = 376°C). As such, the $T_{d,5}$ of the converted atactic poly(D-CamL) from isotactic poly(D-CamL) (Table 1, **Run 1**) is 370°C (Figure S16). The TGA results may be attributed to the tendency of isotactic poly(D-CamL) to depolymerize to the cyclic monomer of D-CamL, while the *trans*-structure present in atactic poly(D-CamL) chains impedes the formation of monomer (Scheme S3). The different thermal properties of the isotactic and atactic poly(D-CamL) further motivated us to investigate the stereocontrolled polymerization of D-CamL.

We next investigated the effects of adding an epimerization inhibitor to the polymerization with $^{t}BuP_4$. Urea, thiourea (TU), and their derivatives are commonly utilized as epimerization inhibitors.[54,55] We evaluated the effects of a series of these compounds on the polymerization of D-CamL catalyzed by $^{t}BuP_4$. Upon polymerization, we found that the binary catalyst system, consisting of $^{t}BuP_4$ and various urea derivatives, allowed for the synthesis of poly(D-CamL) with varied tacticity (*cis*/*trans* ratio), where tacticity could be altered by changing the structure of the urea derivative added. Addition of commercially available carbonyl diamide (urea) and TU were investigated on the polymerization of D-CamL. The addition of urea resulted in a significant decrease in the polymerization rate (37% after 24 h) and a slight increase in the formation of *cis*-repeat units over *trans*- (*cis*/*trans* = 70/30), poly(D-CamL) (Table 1, **Run 4**). The improved *cis*/*trans* ratio indicated that urea slightly suppressed epimerization. Conversely, the addition of TU resulted in no conversion of D-CamL (Table 1, **Run 5**). We hypothesized that the lack of monomer conversion may be attributed to the formation of H-bonding. TU possessing a lower pK_a would form a stronger H-bond with O^- (active chain end) and −C=O (carbonyl group) in the monomer compared with urea (proposed mechanism in Scheme S4). Furthermore, the use of TU combined with $^{t}BuP_4$ results in significant steric hindrance, which

may impede polymerization. Based on these results of using urea and thiourea additives, only urea derivatives were investigated further.

Two commercially available substituted ureas, N,N′-dicyclohexylurea (urea 1) and N,N′-diphenylurea (urea 2), were studied as additives in the polymerization of D-CamL catalyzed by ^{t}BuP$_4$. Upon addition of urea 1 (pK_a = 26.9, Scheme S5), 89% conversion was achieved after 1 h and poly(D-CamL) (M_w = 27.5 kDa, *cis*/*trans* = 60/40, T_m = 161°C, Table 1, **Run 6**, Figure 1C) exhibited a lower *cis*/*trans* ratio and T_m compared with poly(D-CamL) (Table 1, **Run 3**). Upon utilizing urea 2 (pK_a = 20.8, Scheme S5), the resulting poly(D-CamL) (M_w = 16.0 kDa, *cis*/*trans* = 77/23, T_m = 171°C, Table 1, **Run 7**, Figure 1C) had higher tacticity compared with poly(D-CamL) produced using urea 1 (Table 1, **Run 6**), which suggested that the lower pK_a value of the substituted urea additive resulted in reduced epimerization. To test this hypothesis, we further decreased the pK_a of the urea additive by introducing strongly electron-withdrawing groups (−CF_3) at the para (urea 3) and meta (urea 4) positions. The poly(D-CamL)s obtained when adding either urea 3 or urea 4 (Table 1, **Run 8** and Table 1, **Run 9**, respectively) have a higher tacticity (*cis*/*trans* were around 90/10) but at the cost of monomer conversion as less than 50% conversion was observed after 80 h. The decreased monomer conversion and increased tacticity observed when lower pK_a urea derivatives were used may be explained by considering H-bonding between urea and both the O^- and −C=O in the monomer. The urea with lower pK_a will have stronger H-bonding,[56] resulting in reduced reactivity and basicity of O^-. The proposed mechanism is depicted in Scheme S4.

To achieve balance between tacticity and rate of monomer conversion, two asymmetric ureas, N-Cyclohexyl-N′-phenylurea (urea 5) and N-Cyclohexyl-N′-[4-(1,1-dimethylethyl)phenyl]urea (urea 6) were investigated as additives in the polymerization of D-CamL. Consistent with the pK_a value of urea 5 falling between that of urea 1 and urea 2 (Scheme S5), the tacticity of the resulting poly(D-CamL) (M_w = 24.2 kDa, *cis*/*trans* = 67/33, Table 1, **Run 10**) was between that of poly(D-CamL) catalyzed by ^{t}BuP$_4$/urea 1 (Table 1, **Run 6**) and poly(D-CamL) catalyzed by ^{t}BuP$_4$/urea 2 (Table 1, **Run 7**). Additionally, the polymerization catalyzed by ^{t}BuP$_4$/urea 5 reached 96% conversion after 6.0 h, which was also between that of the ^{t}BuP$_4$/urea 1 and ^{t}BuP$_4$/urea 2 catalyzed polymerization. To further decrease the time required to achieve high monomer conversion, an electron-donating group (tert-butyl group, −^{t}Bu) was introduced at the para position of the phenyl group in urea 5, resulting in urea 6. The ^{t}BuP$_4$/urea 6 system resulted in high monomer conversion in decreased reaction time (91% after 3.5 h, Table 1, **Run 11**) compared with ^{t}BuP$_4$/urea 5 (Table 1, **Run 10**). These results demonstrate that a binary system comprising ^{t}BuP$_4$ and urea can be used to prepare poly(D-CamL) with variable tacticity.

Proposed mechanism for the modulation of tacticity

To help further explain the modulation of tacticity when the polymerization of D-CamL is catalyzed by La(N(SiMe$_3$)$_2$)$_3$, ^{t}BuP$_4$, and ^{t}BuP$_4$/urea, we proposed the mechanism shown in Scheme 2. When the ^{t}BuP$_4$ was used to polymerize D-CamL without the addition of a urea, the weak interaction between the O^- and [^{t}BuP$_4$-H]$^+$ enabled facile deprotonation (intra- and inter-chain deprotonation shown in Scheme S2) of the methylene near the carbonyl group, forming a carbanion intermediate through which the *trans*-repeat unit can be formed. With the addition of a urea cocatalyst, H-bonding occurs between the urea, D-CamL, and the O^- on the propagating polymer chain end. H-bonding between O^- and urea stabilizes the O^-, thereby further lowering the probability of carbanion intermediate formation. Therefore, addition of urea would alter the relative quantity of *trans*-repeat

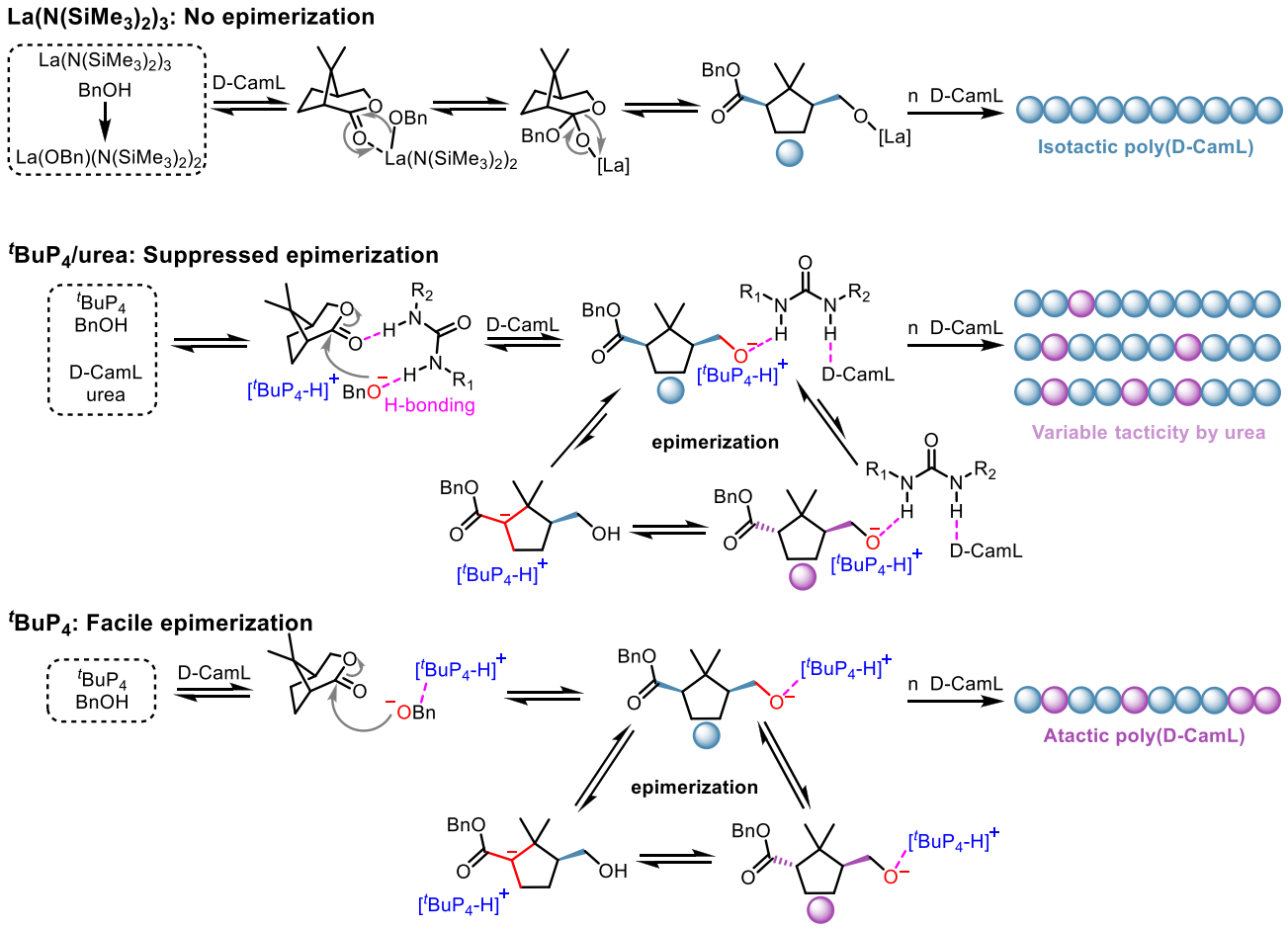

Scheme 2. Proposed mechanism of epimerization in the presence of ^{t}BuP$_4$, ^{t}BuP$_4$/urea, and La(N(SiMe$_3$)$_2$)$_3$

units. In contrast to ^{t}BuP$_4$, the La(N(SiMe$_3$)$_2$)$_3$ would not deprotonate the methylene near the carbonyl group. Therefore, isotactic poly(D-CamL) is obtained by using La(N(SiMe$_3$)$_2$)$_3$.

Material properties of poly(D-CamL)

La(N(SiMe$_3$)$_2$)$_3$, ^{t}BuP$_4$/urea 1, and ^{t}BuP$_4$/urea 6 were chosen as the catalyst systems to prepare larger quantities of poly(D-CamL) required for materials property analysis because these three systems allowed for production of polymers possessing a range of *cis*/*trans* ratios. Poly(D-CamL), catalyzed by ^{t}BuP$_4$/urea 1, ^{t}BuP$_4$/urea 6, and La(NSiMe$_3$)$_2$)$_3$ (Table 2, **Runs 2**, **3**, and **1**, respectively), were obtained and the T_m increased from 169°C to 182°C and 186°C /225°C, respectively (Figure 2A), in accordance with the *cis*/*trans* ratio change from 58/42 to 61/39 to 100/0. We also noticed that the ΔH_f of polymers reported in Table 2 are lower than the ΔH_f of the polymers reported in Table 1. This phenomenon could be attributed to slower rates for crystallization occurring in higher molecular weight polymers due to the reduced mobility of the chain segments; incomplete crystallization leads to reduced ΔH_f.

The mechanical properties of poly(D-CamL) with varying tacticity were investigated by tensile testing of dog-bone-shaped specimens prepared from films produced by

Table 2. Polymerization results of D-CamL with tunable *cis/trans* ratios

Run	Monomer	Catalyst	Conv. (%)[a]	M_w (kDa)[b]	$Đ$[b]	T_g (°C)[c]	T_m (°C)[c]	ΔH_f (J/g)[c]	*cis/trans* (%/%)[d]
1	D-CamL	$La(N(SiMe_3)_2)_3$	41	78.8	1.44	N/A	186/225	19.0	100/0
2	D-CamL	$^tBuP_4$/urea 1	56	48.1	1.45	58	169	24.0	58/42
3	D-CamL	$^tBuP_4$/urea 6	40	79.4	1.57	62	182	15.3	61/39
4	*rac*-CamL	$^tBuP_4$/urea 1	57	78.2	1.67	63	184	18.0	62/38

Conditions: polymerizations were conducted in THF at 50°C, except **Run 1**, which was performed in toluene at 100°C, 12 h duration, the monomer concentration is 1 g CamL in 1.5 mL solvent, and the feed ratio [M]:[I]:[Cat.] = 1,000:1:3 except **Run 1**, which [M]:[I]:[Cat.] = 1,000:1:2.

[a]Monomer conversions were measured by ^{1}H NMR of the crude solution after quenching in $CDCl_3$.

[b]M_w and $Đ$ ($Đ = M_w/M_n$) determined by GPC coupled with light scattering at 40°C in $CHCl_3$.

[c]T_g, T_m, and ΔH_f measured by DSC in the second heating scan at a rate of 10°C min^{-1}.

[d]*cis/trans* ratio measured by ^{13}C NMR in the carbonyl region in $CDCl_3$. Note: all TGA and DSC results can be found in Figures S17–S20.

compression molding and quenched with water cooling. Atactic poly(D-CamL) (M_w = 48.1 kDa, Table 2, **Run 2**) exhibited an ϵ_B, 218% ± 24%, Young's modulus of E = 1.64 ± 0.08 GPa, and a high yield stress of 28.0 ± 2.2 MPa (Figure 2B). These results revealed that atactic poly(D-CamL) catalyzed by $^tBuP_4$/urea 1 was a hard and strong material with moderate ductility, which has higher E and comparable yield stress to HDPE[8] (E = 1.10 GPa, yield stress of around 25 MPa).

The $^tBuP_4$/urea 6 catalyzed poly(D-CamL) (M_w = 79.4 kDa, Table 2, **Run 3**) had a higher tacticity than $^tBuP_4$/urea 1 catalyzed poly(D-CamL) (Table 2, **Run 2**) and exhibited a decreased ϵ_B, 163% ± 22% (Figure 2B). In contrast, the isotactic poly(D-CamL) (M_w = 78.8 kDa, Table 2, **Run 1**) catalyzed by $La(N(SiMe_3)_2)_3$ was brittle; the ϵ_B was only 6% ± 2%, but the yield stress was notably high at 33.8 ± 2.7 MPa (Figure 2B). Overall, the results of the tensile testing for poly(D-CamL) indicate that isotactic poly(D-CamL) has the highest yield stress but the lowest ϵ_B, while atactic poly(D-CamL) has a higher ϵ_B for greater ductility.

The WAXD (wide-angle X-ray diffraction, Figure 2C) revealed one main peak at 2θ = 15.6° for atactic poly(D-CamL) (Table 2, **Run 2**), whereas WAXD of atactic poly(D-CamL) (Table 2, **Run 3**) exhibited a shoulder peak at 2θ = 16.6° because of the increased *cis/trans* ratio. Notably, the isotactic poly(D-CamL) (Table 2, **Run 1**) showed two main peaks at 2θ = 15.6° and 16.6°. The lack of the peak at 2θ = 16.6° of atactic poly(D-CamL) (Table 2, **Run 2**) could be explained by crystal defects in atactic poly(D-CamL) arising from chain disorder.[57] As a result, the isotactic poly(D-CamL) has increased crystallinity, which could be further supported by the differential scanning calorimetry (DSC) experiments, with the second heating scans performed at different heating rates (2.5°C/min, 10°C/min, and 20°C/min) (Figure S21). The DSC results showed a decrease in the area (ΔH_f value) of the higher T_m peak with increasing the heating rate, suggesting the formation of a more ordered and thicker crystallization zone after the lower T_m, resulting in the appearance of a higher T_m in isotactic poly(D-CamL). Significantly, regardless of tacticity, based on WAXD and DSC results, we observed intrinsic crystallinity in all poly(D-CamL) samples. This unique property is not common in polyesters and may be imparted by the cyclopentylene and gem-dimethyl structures in the polymer chain.[28,29] Additionally, the circular dichroism (CD) spectra (Figure S22) of isotactic poly(D-CamL) (Table 2, **Run 1**) and atactic poly(D-CamL) (Table 2, **Run 2**) were obtained. Isotactic poly(D-CamL) showed a stronger positive Cotton effect than the atactic poly(D-CamL), which confirmed that the isotactic poly(D-CamL) showed higher optical activity than the atactic poly(D-CamL). The atactic sample also exhibited a rather weak positive Cotton effect, supporting our conclusion that the atactic poly(D-CamL) has a decreased *cis/trans* ratio of

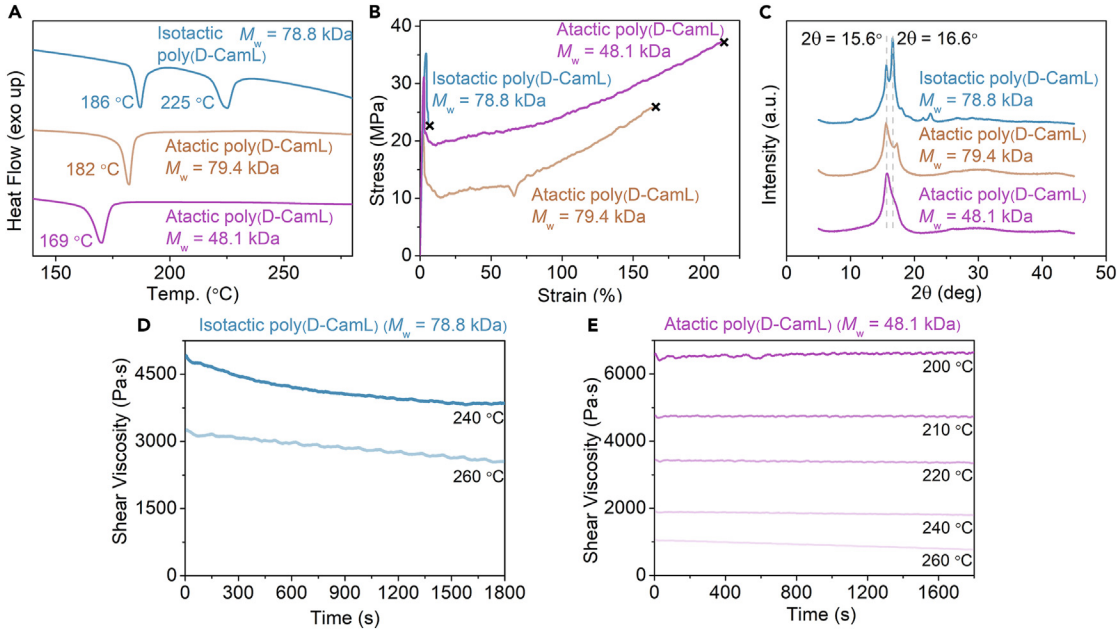

Figure 2. Thermal, mechanical, wide-angle X-ray diffraction, and rheology characterization results of poly(D-CamL)

(A) DSC curves of the poly(D-CamL).

(B) Representative stress-strain curves of the poly(D-CamL), extension rate = 5 mm/min, ambient condition.

(C) WAXD plots of the poly(D-CamL).

(D and E) Shear viscosity plots ($\dot{\gamma}$ = 0.5 s^{-1}) in melt of isotactic poly(D-CamL) (M_w = 78.8 kDa) and atactic poly(D-CamL) (M_w = 48.1 kDa).

58/42 compared with the isotactic poly(D-CamL), which has a *cis*/*trans* ratio of 100/0.

Thermomechanical properties of isotactic poly(D-CamL) (Table 2, **Run 1**) and atactic poly(D-CamL) (Table 2, **Run 2**) were evaluated using dynamic mechanical analysis (DMA) in a tension film mode (Figure S23). Isotactic poly(D-CamL) (Table 2, **Run 1**) exhibited a slightly higher storage modulus of E' = 3,289 MPa than atactic poly(D-CamL) (Table 2, **Run 2**) of E' = 3,135 MPa in the glassy state. After the glass-transition region with an alpha transition (T_α = 86°C and T_α = 75°C, respectively, defined by the peak maxima of tanδ, E''/E'), E' of isotactic and atactic poly(D-CamL) decreased by about one order of magnitude after T_α, meaning that these materials still maintain a relatively high storage moduli in the rubbery state.

To evaluate the stability of these polymers to thermal processing, rheological experiments were performed using a continuous flow study at a shear rate of 0.5 s^{-1}. The temporal changes in shear viscosity for both isotactic poly(D-CamL) (Table 2, **Run 1**) and atactic poly(D-CamL) (Table 2, **Run 2**) were monitored at temperatures surpassing T_m (Figures 2D and 2E). The shear viscosity of atactic poly(D-CamL) (Table 2, **Run 2**) remained nearly constant without any noticeable decline for 30 min when exposed to temperatures ranging from 200°C to 240°C. Upon heating for 30 min at 260°C, the shear viscosity decreased from 1,063 to 769 Pa•s, while the isotactic poly(D-CamL) (Table 2, **Run 1**) showed a decrease in shear viscosity, from 4,908 to 3,850 Pa•s upon heating for 30 min at 240°C. These results demonstrated the thermal processability of atactic poly(D-CamL) (Table 2, **Run 2**) but not isotactic poly(D-CamL) (Table 2, **Run 1**). The shear thinning experiment (Figure S24) also showed a rapid decrease in viscosity of atactic poly(D-CamL) (Table 2, **Run 2**)

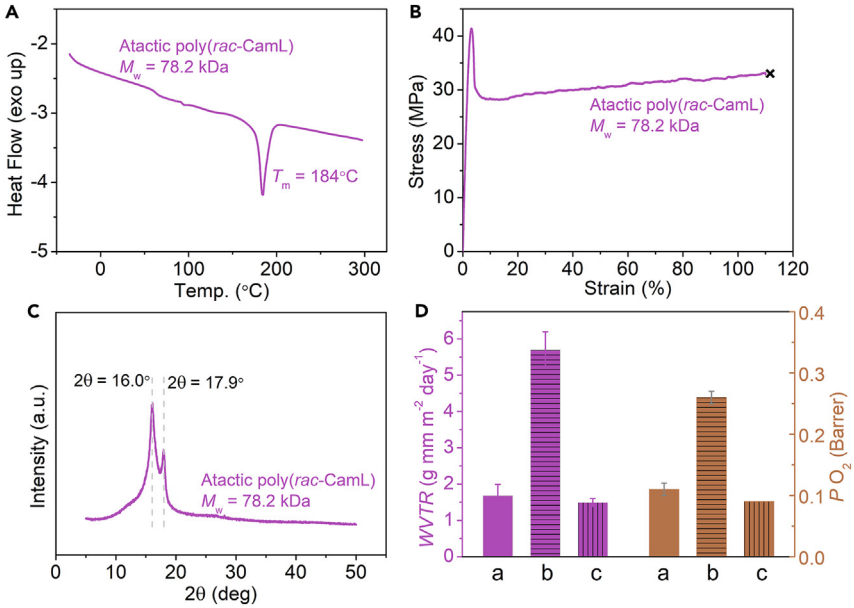

Figure 3. Thermal, mechanical, WAXD, and permeability characterization results of atactic poly(*rac*-CamL)

(A) DSC trace of poly(*rac*-CamL).

(B) Representative stress-strain curve of the atactic poly(*rac*-CamL), extension rate = 5 mm/min, ambient condition.

(C) WAXD of the poly(*rac*-CamL).

(D) Water vapor transmission rate and oxygen permeability of poly(*rac*-CamL) (a, M_w = 78.2 kDa), PLLA (b, M_w = 162 kDa), and PET (c, intrinsic viscosity of 0.80 dL g^{-1} in *m*-cresol).

upon its exposure to sheer strain, which is a characteristic that enhances polymer processability.

Syndiotactic-rich polymers from *rac*-CamL

D-CamL used in the experiments described thus far was synthesized from natural camphor. In contrast with natural camphor, synthetic camphor is typically available as a racemic mixture. Given the prevalence of racemic camphor, we sought to examine the properties of polymers derived from a racemic mixture. The racemic monomer, *rac*-CamL, was synthetized according to a similar procedure to the one used to synthesize D-CamL (Scheme S1).

Atactic poly(*rac*-CamL) (M_w = 78.2 kDa, Table 2, **Run 4**) was synthesized using ^{t}BuP$_4$/urea 1 for mechanical testing. The *cis*/*trans* ratio of atactic poly(*rac*-CamL) was 62/38 and the T_m was 184°C (Figure 3A; Table 2, **Run 4**,). Tensile testing (Figure 3B) revealed a notably higher yield stress of nearly 40 MPa and ϵ_B, 121% ± 9% than that of isotactic poly(D-CamL) (Table 2, **Run 1**). Upon WAXD analysis (Figure 3C), atactic poly(*rac*-CamL) exhibited two distinct sharp peaks at 2θ = 16.0° and 17.9°, which showed a slight shift in comparison to isotactic poly(D-CamL), indicating that atactic poly(*rac*-CamL) may crystallize differently than poly(D-CamL). ^{13}C NMR analysis revealed that atactic poly(*rac*-CamL) (M_w = 78.2 kDa) has a higher proportion of D-L linkages at 173.65 ppm than D-D/L-L linkages at 173.59 ppm (Figure S25), indicating that atactic poly(*rac*-CamL) tends to be syndiotactic-rich. The discrepancy between D-L linkage content in atactic and isotactic poly(*rac*-CamL) may be caused by the larger counterion ([^{t}BuP$_4$-H]$^+$) at the polymer chain ends leading to alternating D-L insertion, whereas the La(N(SiMe$_3$)$_2$)$_3$ does not have this same effect.

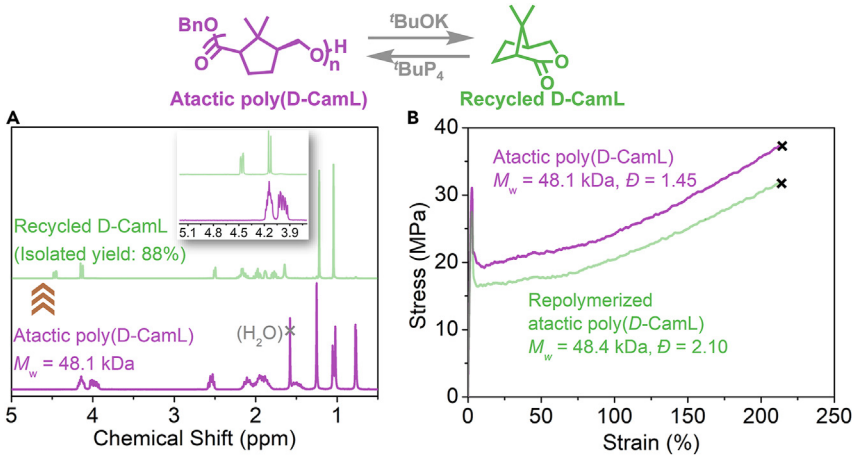

Figure 4. ^{1}H NMR and mechanical characterization results of depolymerization of atactic poly(D-CamL) and repolymerization of recycled D-CamL

(A) ^{1}H NMR ($CDCl_3$, 23°C) spectra of the poly(D-CamL) (M_w = 48.1 kDa) and recycled D-CamL. Inset: enlarged area from 5.2 to 3.7 ppm.

(B) Representative stress-strain curves of the poly(D-CamL) (M_w = 48.1 kDa) and the repolymerized poly(D-CamL) (M_w = 48.4 kDa).

To assess the potential of poly(CamL) for use as a packaging material, we conducted barrier property tests on syndiotactic-rich poly(*rac*-CamL) (Table 2, **Run 4**). Syndiotactic-rich poly(*rac*-CamL) demonstrates a relatively low water vapor transmission rate (WVTR) of 1.68 ± 0.31 (g mm m^{-2} day^{-1}), and an outstanding *P* O_2 character of 0.11 ± 0.01 Barrer. Desirable barrier properties are likely attributable to the polymer's T_g being above room temperature (63°C) and semicrystalline in nature. Both the *WVTR* and *P* O_2 are much lower than that of commercial PLLA and approach that of commercial polyethylene terephthalate (PET), which is widely used in packaging materials (Figure 3D)[19,58,59]; these results demonstrate that syndiotactic-rich poly(*rac*-CamL) could be suitable for use as a packaging material.

Chemical recyclability and repolymerization

To investigate the thermodynamics of the D-CamL polymerization, the change in enthalpy (ΔH°_p), change in entropy (ΔS°_p), and $T_{ceiling}$ were measured. The equilibrium monomer concentration was determined at varied temperatures and plotted as a function of temperature to yield a van 't Hoff plot (Figure S26). This analysis provided the thermodynamic parameters (ΔH°_p = −21.0 kJ mol^{-1}, ΔS°_p = −55.5 J mol^{-1} K^{-1}), while the $T_{ceiling}$ at $[M]_0$ = 1.0 M was determined to be 381 K (105°C). The low $T_{ceiling}$ value suggested that poly(D-CamL) could be depolymerized to D-CamL at elevated temperature.

Due to the epimerization observed during polymerization, we hypothesized that a sufficiently strong base would be necessary to support the onset of epimerization during depolymerization and achieve recovery of D-CamL from atactic poly(D-CamL). Based on this hypothesis, ^{t}BuOK was selected to depolymerize atactic poly(D-CamL) (Table 2, **Run 2**). Atactic poly(D-CamL), which was homogeneously mixed with ^{t}BuOK, was successfully converted to D-CamL (shown in Figure 4A) in 88% isolated yield in a sublimator at 200°C and 200 millitorr. The recovered D-CamL was successfully polymerized again using $^{t}BuP_4$/urea 1, forming poly(D-CamL) (48.4 kDa) with mechanical properties comparable to virgin poly(D-CamL) (Figure 4B), demonstrating successful closed-loop recycling.

Conclusions

Through combining hybridization and gem-dialkyl substitution strategies, a camphor-derived, high-performance aliphatic polyester was efficiently synthesized and selectively depolymerized back to monomer in high isolated yield. The ROP of CamL was catalyzed by a La complex, superbase, or a superbase/urea binary catalyst system; these different catalyst systems allowed for the preparation of isotactic, atactic, and syndiotactic-rich poly(CamL) materials from the optically pure or racemic monomer. Variation in polymer tacticity modulates materials properties such as T_m, ductility, yield stress, and Young's modulus. Thermal and mechanical characterization demonstrated that poly(CamL) exhibits comparable and/or enhanced properties compared with PLA, including similar T_m, T_g, and comparable yield stress, while exhibiting better ductility and intrinsic crystallinity. Furthermore, low WVTR and low $P O_2$ character confirmed that poly(CamL) has the potential to be used as packaging material. Above all, this combination strategy produced a polymer that not only showcases the potential of bio-based polymers in reducing reliance on fossil fuels but also emphasizes the importance of recyclability and performance in the development of next-generation plastics.

EXPERIMENTAL PROCEDURES

Resource availability

Lead contact

Requests for further information should be directed to and will be fulfilled by the lead contact, Garret M. Miyake (garret.miyake@colostate.edu).

Materials availability

All reagents used in this study and full experimental details can be found in the supplemental information.

Data and code availability

All data needed to evaluate the conclusions in the paper are present in the paper and/or the supplemental information.

SUPPLEMENTAL INFORMATION

Supplemental information can be found online at https://doi.org/10.1016/j.chempr.2024.05.024.

ACKNOWLEDGMENTS

This work was supported by RePLACE (Redesigning Polymers to Leverage a Circular Economy) funded by the Office of Science of the US Department of Energy through award no. DE-SC0022290, the National Institutes of Health under award no. R35GM144356, Basque Country Government (GC IT 1667-22), and Colorado State University. The authors thank the Analytical Resources Core (RRID: SCR_021758) at Colorado State University for instrument access and training and thank Jason Boes and Alan Kennan for assistance with CD experimentation. G.M.M. acknowledges support from the Camille & Henry Dreyfus Foundation through a Camille Dreyfus Teacher-Scholar Award.

AUTHOR CONTRIBUTIONS

Z.H. and G.M.M. conceived the idea and designed the experiments. Z.H. and S.N.B. carried out the experiments. Z.H., S.N.B., and G.M.M. co-wrote the manuscript. All authors participated in data analysis, discussions, and editing the manuscript. G.M.M. directed the project.

DECLARATION OF INTERESTS

The authors declare no competing interests.

Received: March 11, 2024
Revised: May 3, 2024
Accepted: May 31, 2024
Published: June 26, 2024

REFERENCES

1. Jambeck, J.R., Geyer, R., Wilcox, C., Siegler, T.R., Perryman, M., Andrady, A., Narayan, R., and Law, K.L. (2015). Marine pollution. Plastic Waste Inputs from Land into the Ocean. Science *347*, 768–771. https://doi.org/10.1126/science.1260352.

2. MacLeod, M., Arp, H.P.H., Tekman, M.B., and Jahnke, A. (2021). The Global Threat from Plastic Pollution. Science *373*, 61–65. https://doi.org/10.1126/science.abg5433.

3. Schyns, Z.O.G., and Shaver, M.P. (2021). Mechanical Recycling of Packaging Plastics: A Review. Macromol. Rapid Commun. *42*, e2000415. https://doi.org/10.1002/marc.202000415.

4. Kumar, R., Sadeghi, K., Jang, J., and Seo, J. (2023). Mechanical, Chemical, and Bio-recycling of Biodegradable Plastics: A Review. Sci. Total Environ. *882*, 163446. https://doi.org/10.1016/j.scitotenv.2023.163446.

5. Jehanno, C., Alty, J.W., Roosen, M., De Meester, S., Dove, A.P., Chen, E.Y.X., Leibfarth, F.A., and Sardon, H. (2022). Critical Advances and Future Opportunities in Upcycling Commodity Polymers. Nature *603*, 803–814. https://doi.org/10.1038/s41586-021-04350-0.

6. Coates, G.W., and Getzler, Y.D.Y.L. (2020). Chemical Recycling to Monomer for An Ideal, Circular Polymer Economy. Nat. Rev. Mater. *5*, 501–516. https://doi.org/10.1038/s41578-020-0190-4.

7. Nicholson, S.R., Rorrer, J.E., Singh, A., Konev, M.O., Rorrer, N.A., Carpenter, A.C., Jacobsen, A.J., Román-Leshkov, Y., and Beckham, G.T. (2022). The Critical Role of Process Analysis in Chemical Recycling and Upcycling of Waste Plastics. Annu. Rev. Chem. Biomol. Eng. *13*, 301–324. https://doi.org/10.1146/annurev-chembioeng-100521-085846.

8. Zhao, Y., Rettner, E.M., Harry, K.L., Hu, Z., Miscall, J., Rorrer, N.A., and Miyake, G.M. (2023). Chemically Recyclable Polyolefin-like Multiblock Polymers. Science *382*, 310–314. https://doi.org/10.1126/science.adh3353.

9. Shi, C., Quinn, E.C., Diment, W.T., and Chen, E.Y.X. (2024). Recyclable and (Bio)degradable Polyesters in a Circular Plastic Economy. Chem. Rev. *124*, 4393–4478. https://doi.org/10.1021/acs.chemrev.3c00848.

10. Schwab, S.T., Baur, M., Nelson, T.F., and Mecking, S. (2024). Synthesis and Deconstruction of Polyethylene-type Materials. Chem. Rev. *124*, 2327–2351. https://doi.org/10.1021/acs.chemrev.3c00587.

11. Zhu, Y., Romain, C., and Williams, C.K. (2016). Sustainable Polymers from Renewable Resources. Nature *540*, 354–362. https://doi.org/10.1038/nature21001.

12. Abdelshafy, A., Hermann, A., Herres-Pawlis, S., and Walther, G. (2023). Opportunities and Challenges of Establishing a Regional Bio-based Polylactic Acid Supply Chain. Glob. Chall. *7*, 2200218. https://doi.org/10.1002/gch2.202200218.

13. Jamshidian, M., Tehrany, E.A., Imran, M., Jacquot, M., and Desobry, S. (2010). Poly-Lactic Acid: Production, Applications, Nanocomposites, and Release Studies. Compr. Rev. Food Sci. Food Saf. *9*, 552–571. https://doi.org/10.1111/j.1541-4337.2010.00126.x.

14. Gallin, C.F., Lee, W.-W., and Byers, J.A. (2023). A Simple, Selective, and General Catalyst for Ring Closing Depolymerization of Polyesters and Polycarbonates for Chemical Recycling. Angew. Chem. Int. Ed. Engl. *62*, e202303762. https://doi.org/10.1002/anie.202303762.

15. McGuire, T.M., Buchard, A., and Williams, C. (2023). Chemical Recycling of Commercial Poly(L-lactic acid) to L-Lactide Using a High-Performance Sn(II)/Alcohol Catalyst System. J. Am. Chem. Soc. *145*, 19840–19848. https://doi.org/10.1021/jacs.3c05863.

16. Garlotta, D. (2001). A Literature Review of Poly(Lactic Acid). J. Polym. Environ. *9*, 63–84. https://doi.org/10.1023/A:1020200822435.

17. Naser, A.Z., Deiab, I., and Darras, B.M. (2021). Poly(lactic acid) (PLA) and Polyhydroxyalkanoates (PHAs), Green Alternatives to Petroleum-based Plastics: A Review. RSC Adv. *11*, 17151–17196. https://doi.org/10.1039/d1ra02390j.

18. Chile, L.E., Mehrkhodavandi, P., and Hatzikiriakos, S.G. (2016). A Comparison of the Rheological and Mechanical Properties of Isotactic, Syndiotactic, and Heterotactic Poly(lactide). Macromolecules *49*, 909–919. https://doi.org/10.1021/acs.macromol.5b02568.

19. Sangroniz, A., Zhu, J.-B., Tang, X., Etxeberria, A., Chen, E.Y.-X., and Sardon, H. (2019). Packaging Materials with Desired Mechanical and Barrier Properties and Full Chemical Recyclability. Nat. Commun. *10*, 3559. https://doi.org/10.1038/s41467-019-11525-x.

20. Mohan, S., and Panneerselvam, K. (2022). A Short Review on Mechanical and Barrier Properties of Polylactic Acid-based Films. Mater. Today: Proc. *56*, 3241–3246. https://doi.org/10.1016/j.matpr.2021.09.375.

21. Abel, B.A., Snyder, R.L., and Coates, G.W. (2021). Chemically Recyclable Thermoplastics from Reversible-deactivation Polymerization of Cyclic Acetals. Science *373*, 783–789. https://doi.org/10.1126/science.abh0626.

22. Hester, H.G., Abel, B.A., and Coates, G.W. (2023). Ultra-High-Molecular-Weight Poly(Dioxolane): Enhancing the Mechanical Performance of a Chemically Recyclable Polymer. J. Am. Chem. Soc. *145*, 8800–8804. https://doi.org/10.1021/jacs.3c01901.

23. Shi, C., Reilly, L.T., Phani Kumar, V.S., Coile, M.W., Nicholson, S.R., Broadbelt, L.J., Beckham, G.T., and Chen, E.Y.X. (2021). Design Principles for Intrinsically Circular Polymers with Tunable Properties. Chem *7*, 2896–2912. https://doi.org/10.1016/j.chempr.2021.10.004.

24. Li, X.L., Clarke, R.W., Jiang, J.Y., Xu, T.Q., and Chen, E.Y.X. (2023). A Circular Polyester Platform based on Simple gem-Disubstituted Valerolactones. Nat. Chem. *15*, 278–285. https://doi.org/10.1038/s41557-022-01077-x.

25. Jung, M.E., and Piizzi, G. (2005). gem-Disubstituent Effect: Theoretical Basis and Synthetic Applications. Chem. Rev. *105*, 1735–1766. https://doi.org/10.1021/cr940337h.

26. Bachrach, S.M. (2008). The gem-Dimethyl Effect Revisited. J. Org. Chem. *73*, 2466–2468. https://doi.org/10.1021/jo702665r.

27. Zhou, Z., LaPointe, A.M., Shaffer, T.D., and Coates, G.W. (2023). Nature-inspired Methylated Polyhydroxybutyrates from C1 and C4 Feedstocks. Nat. Chem. *15*, 856–861. https://doi.org/10.1038/s41557-023-01187-0.

28. Zhou, L., Zhang, Z., Shi, C., Scoti, M., Barange, D.K., Gowda, R.R., and Chen, E.Y.X. (2023). Chemically Circular, Mechanically Tough, and Melt-processable Polyhydroxyalkanoates. Science *380*, 64–69. https://doi.org/10.1126/science.adg4520.

29. Shi, C., McGraw, M.L., Li, Z.-C., Cavallo, L., Falivene, L., and Chen, E.Y.-X. (2020). High-performance pan-tactic Polythioesters with Intrinsic Crystallinity and Chemical Recyclability. Sci. Adv. *6*, eabc0495. https://doi.org/10.1126/sciadv.abc0495.

30. Shi, C., Li, Z.-C., Caporaso, L., Cavallo, L., Falivene, L., and Chen, E.Y.-X. (2021). Hybrid Monomer Design for Unifying Conflicting Polymerizability, Recyclability, and Performance Properties. Chem *7*, 670–685. https://doi.org/10.1016/j.chempr.2021.02.003.

31. Shi, C., Clarke, R.W., McGraw, M.L., and Chen, E.Y.X. (2022). Closing the "One Monomer-Two Polymers-One Monomer" Loop via Orthogonal (De)polymerization of a Lactone/Olefin Hybrid. J. Am. Chem. Soc. *144*, 2264–2275. https://doi.org/10.1021/jacs.1c12278.

32. Shi, C., Reilly, L.T., and Chen, E.Y.X. (2023). Hybrid Monomer Design Synergizing Property Trade-offs in Developing Polymers for Circularity and Performance. Angew. Chem. Int. Ed. Engl. *62*, e202301850. https://doi.org/10.1002/anie.202301850.

33. Zielińska-Błajet, M., and Feder-Kubis, J. (2020). Monoterpenes and Their Derivatives-Recent Development in Biological and Medical Applications. Int. J. Mol. Sci. *21*, 7078. https://doi.org/10.3390/ijms21197078.

34. Masyita, A., Mustika Sari, R., Dwi Astuti, A., Yasir, B., Rahma Rumata, N., Emran, T.B., Nainu, F., and Simal-Gandara, J. (2022). Terpenes and Terpenoids as Main Bioactive Compounds of Essential Oils, Their Roles in Human Health and Potential Application as Natural Food Preservatives. Food Chem. X *13*, 100217. https://doi.org/10.1016/j.fochx.2022.100217.

35. Lu, J., Kamigaito, M., Sawamoto, M., Higashimura, T., and Deng, Y.-X. (1997). Living Cationic Isomerization Polymerization of β-Pinene. 1. Initiation with HCl−2-Chloroethyl Vinyl Ether Adduct/$TiCl_3(O^iPr)$ in Conjunction with $^nBu_4NCl$. Macromolecules *30*, 22–26. https://doi.org/10.1021/ma960118t.

36. Lowe, J.R., Martello, M.T., Tolman, W.B., and Hillmyer, M.A. (2011). Functional Biorenewable Polyesters from Carvone-derived Lactones. Polym. Chem. *2*, 702–708. https://doi.org/10.1039/C0PY00283F.

37. Satoh, K., Nakahara, A., Mukunoki, K., Sugiyama, H., Saito, H., and Kamigaito, M. (2014). Sustainable Cycloolefin Polymer from Pine Tree Oil for Optoelectronics Material: Living Cationic Polymerization of β-Pinene and Catalytic Hydrogenation of High-Molecular-Weight Hydrogenated Poly(β-Pinene). Polym. Chem. *5*, 3222–3230. https://doi.org/10.1039/C3PY01320K.

38. Hillmyer, M.A., and Tolman, W.B. (2014). Aliphatic Polyester Block Polymers: Renewable, Degradable, and Sustainable. Acc. Chem. Res. *47*, 2390–2396. https://doi.org/10.1021/ar500121d.

39. Winnacker, M., and Rieger, B. (2015). Recent Progress in Sustainable Polymers Obtained From Cyclic Terpenes: Synthesis, Properties, and Application Potential. ChemSusChem *8*, 2455–2471. https://doi.org/10.1002/cssc.201500421.

40. Roth, S., Funk, I., Hofer, M., and Sieber, V. (2017). Chemoenzymatic Synthesis of a Novel Borneol-Based Polyester. ChemSusChem *10*, 3574–3580. https://doi.org/10.1002/cssc.201701146.

41. Winnacker, M. (2018). Pinenes: Abundant and Renewable Building Blocks for a Variety of Sustainable Polymers. Angew. Chem. Int. Ed. Engl. *57*, 14362–14371. https://doi.org/10.1002/anie.201804009.

42. Luo, Y.-C., Zhang, H.-H., Wang, Y., and Xu, P.-F. (2010). Synthesis of α-Amino Acids Based on Chiral Tricycloiminolactone Derived from Natural (+)-Camphor. Acc. Chem. Res. *43*, 1317–1330. https://doi.org/10.1021/ar100050p.

43. Chen, W., Vermaak, I., and Viljoen, A. (2013). Camphor–a fumigant during the Black Death and a coveted fragrant wood in ancient Egypt and Babylon–a review. Molecules *18*, 5434–5454. https://doi.org/10.3390/molecules18055434.

44. Roth, S. (2020). Biotransformation of Camphor-Derivatives for the Synthesis of Bio-based Polymers (Technische Universität München).

45. Mossa, J.S., and Hassan, M.M.A. (1984). Camphor. In Analytical Profiles of Drug Substances, K. Florey, ed. (Academic Press), pp. 27–93. https://doi.org/10.1016/S0099-5428(08)60188-4.

46. Pang, C., Jiang, X., Yu, Y., Chen, L., Ma, J., and Gao, H. (2019). Copolymerization of Natural Camphor-Derived Rigid Diol with Various Dicarboxylic Acids: Access to Biobased Polyesters with Various Properties. ACS Macro Lett. *8*, 1442–1448. https://doi.org/10.1021/acsmacrolett.9b00570.

47. Nsengiyumva, O., and Miller, S.A. (2019). Synthesis, Characterization, and Water-degradation of Biorenewable Polyesters Derived from Natural Camphoric Acid. Green Chem. *21*, 973–978. https://doi.org/10.1039/C8GC03990A.

48. Jiang, B., and Thomas, C.M. (2023). Efficient Synthesis of Camphor-based Polycarbonates: A Direct Route to Recyclable Polymers. Catal. Sci. Technol. *13*, 3910–3915. https://doi.org/10.1039/D3CY00423F.

49. Robert, C., de Montigny, F., and Thomas, C.M. (2011). Tandem synthesis of alternating polyesters from renewable resources. Nat. Commun. *2*, 586. https://doi.org/10.1038/ncomms1596.

50. Xie, H., Feng, J., Yang, X., Zhao, Y., Song, P., Wang, H., and Xu, Z. (2022). One-pot Sequence-selective Synthesis of Polylactone-containing Block Terpolymers Based on Renewable Terpenoid-derived Monomer and A Simple Organocatalyst. J. Polym. Sci. *60*, 2889–2898. https://doi.org/10.1002/pol.20220188.

51. Boileau, S., and Illy, N. (2011). Activation in Anionic Polymerization: Why Phosphazene Bases are very Exciting Promoters. Prog. Polym. Sci. *36*, 1132–1151. https://doi.org/10.1016/j.progpolymsci.2011.05.005.

52. Hong, M., and Chen, E.Y.X. (2016). Towards Truly Sustainable Polymers: A Metal-Free Recyclable Polyester from Biorenewable Non-Strained γ-Butyrolactone. Angew. Chem. Int. Ed. Engl. *55*, 4188–4193. https://doi.org/10.1002/anie.201601092.

53. Liu, S., Ren, C., Zhao, N., Shen, Y., and Li, Z. (2018). Phosphazene Bases as Organocatalysts for Ring-Opening Polymerization of Cyclic Esters. Macromol. Rapid Commun. *39*, e1800485. https://doi.org/10.1002/marc.201800485.

54. Lin, B., and Waymouth, R.M. (2017). Urea Anions: Simple, Fast, and Selective Catalysts for Ring-Opening Polymerizations. J. Am. Chem. Soc. *139*, 1645–1652. https://doi.org/10.1021/jacs.6b11864.

55. Li, M., Tao, Y., Tang, J., Wang, Y., Zhang, X., Tao, Y., and Wang, X. (2019). Synergetic Organocatalysis for Eliminating Epimerization in Ring-Opening Polymerizations Enables Synthesis of Stereoregular Isotactic Polyester. J. Am. Chem. Soc. *141*, 281–289. https://doi.org/10.1021/jacs.8b09739.

56. Wang, X., and Hadjichristidis, N. (2020). Poly(amine-co-ester)s by Binary Organocatalytic Ring-Opening Polymerization of N-Boc-1,4-oxazepan-7-one: Synthesis, Characterization, and Self-Assembly. Macromolecules *53*, 223–232. https://doi.org/10.1021/acs.macromol.9b02084.

57. Van der Meer, D.-W. (2003). Structure-Property Relationships in Isotactic Polypropylene (University of Twente).

58. Marsh, K., and Bugusu, B. (2007). Food Packaging—Roles, Materials, and Environmental Issues. J. Food Sci. *72*, R39–R55. https://doi.org/10.1111/j.1750-3841.2007.00301.x.

59. Sangroniz, A., haos, A., Iriarte, M., del Río, J., Sarasua, J.-R., and Etxeberria, A. (2018). Influence of the Rigid Amorphous Fraction and Crystallinity on Polylactide Transport Properties. Macromolecules *51*, 3923–3931. https://doi.org/10.1021/acs.macromol.8b00833.